Method for the Calculation of Mutual Coupling Between Discontinuities in Planar Circuits

Bart L. A. Van Thielen and Guy A. E. Vandenbosch, *Member, IEEE*

***Abstract*—In this paper, a fast method for the calculation of mutual coupling between discontinuities is described. The discontinuities must be small compared to the wavelength and compared to the distance between them. For most circuits, these assumptions are valid. Under these circumstances, the component's (discontinuity) radiation behavior can be accurately modeled by using adequately placed dipoles. This method uses far less unknowns than the method of moments. If the distances between the components become smaller or the components become bigger, then the accuracy can be improved by using more dipoles.**

***Index Terms*—CAD, EMC, mutual coupling.**

I. Introduction

As MODERN circuits become smaller and the frequencies that they work at become higher, parasitic coupling within the circuits will inevitably start to influence the behavior of the circuit more and more. Therefore, it is necessary to include the influence of mutual coupling in the circuit simulators that are used to design the circuit. The methods that are currently being used to analyze mutual coupling in circuits need a lot of computer memory and time to solve the circuit. This is because they subdivide the whole circuit into rooftops, calculate all the inter-rooftop couplings, and use these couplings to calculate the current of the rooftops by solving a huge set of equations (i.e., the moment method).

A planar circuit can generally be regarded as being composed of discontinuities and transmission lines connecting these discontinuities. This paper will describe a new method, which involves calculating mutual coupling between the discontinuities of the circuit instead of segmenting and solving the whole circuit at once. The described method will become one of the modules of an overall model for the calculation of mutual coupling in planar circuits. Other modules will handle the couplings between transmission lines, from transmission lines to discontinuities, and vice versa.

Discontinuities are either components (resistors, capacitors, transistors, etc.) or metal (microstrip) structures (T-junction, corner, open stub, etc.). No distinction will be made between these two types of discontinuities in the remainder of this paper.

The key assumption of the new method is that, if the discontinuities are small compared to the wavelength and distance between them is large compared to their size, their radiation behavior can be modeled as that of an elementary dipole. More than one dipole can be used per discontinuity if the above-mentioned assumptions are not met. Another assumption is that the current on one discontinuity is only slightly influenced by the other discontinuities in its vicinity (higher order coupling is neglected). This is true if the coupling levels between the discontinuities remain lower than about -7 dB. Discontinuities (components) that are coupled tighter than this must be taken together to form a new component. The relationship between currents and fields on the dipoles and incoming and outgoing transmission line waves, respectively, is described by an extension to the S-parameter model of the discontinuity.

In this paper, the results of the developed method are compared with those of a standard method of moments (MoM). The theory and corresponding software that implements this standard method are described in [1]–[4]. Other methods to solve the problem of mutual coupling in circuits are the expansion wave concept [5] and the fast multipole method [6]. The two main differences of the described method with [5] and [6] are as follows.

1) The method that is presented here is a library-based modular approach: the S-parameters and dipole position and excitation data are stored in model files for each discontinuity. [5] and [6] do not split the circuit up into its (separately solved) components, but solve it entirely, not taking advantage of the specific properties (S-parameters and known current distributions) of its components.
2) The method that is proposed here only takes "first-order coupling" into account. Higher order coupling (indirect coupling between two components through reflections of incident fields at others) is neglected. This results in a further speed increase, while the results remain accurate enough if the components are not tighter coupled than -7 dB (see above), which is the true for most circuits.

Due to these two differences, the new method is much faster and needs less memory than [5] and [6].

II. Dipole Equivalent of a Current Distribution

In this section, we will describe how, under certain conditions, a current distribution can be replaced by dipoles that generate approximately the same field distribution as the original current distribution.

To rigorously calculate the field that a current distribution generates, this distribution must be convolved with the appropriate Green's function.

A possible simplification is to approximate the current distribution by three elementary dipoles, oriented along the x-, y-, and z-axis. The dipoles are currents flowing in an elementary

Manuscript received September 4, 2000. This work was supported by a scholarship from the Flemish Institute for the Advancement of Scientific-Technological Research in Industry.

The authors are with the Microwave Sections, Katholieke Universiteit Leuven, B-3000 Leuven, Belgium.

Publisher Item Identifier S 0018-9480(02)00743-3.

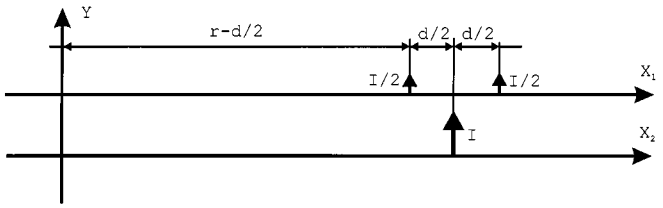

Fig. 1. Current distribution (X_1-axis) and its equivalent (X_2-axis) placed at its current center.

volume dV_d: dV_dI_{xd}, dV_dI_{yd}, and dV_dI_{zd}. I_{xd} is the current density of the x-directed dipole and V_d is its volume. These dipoles are placed in the "current center" of the current distribution. For the x-oriented dipole, this center is given by

$$x_d = \frac{\iiint_v xI_x dxdydz}{\iiint_v I_x dxdydz}$$
$$y_d = \frac{\iiint_v yI_x dxdydz}{\iiint_v I_x dxdydz}$$
$$z_d = \frac{\iiint_v zI_x dxdydz}{\iiint_v I_x dxdydz} \tag{1}$$

where I_x is the current density of the x-oriented current. The product dV_dI_d must be equal to the total integrated current of the original current distribution

$$I_{xd}dV_d = \iiint_v I_x dxdydz. \tag{2}$$

The reason why this dipole will not generate a field that is identical to that of the original current distribution is explained below.

The relation between the field in an observation point and the distance (r) to the current generating this field is given by the appropriate Green's function. It is, in general, mainly a mixture of $1/\sqrt{r}$ (surface wave) and $1/r$, $1/r^2$ (space wave) dependencies, as described in [4]. Suppose that we only have a $1/r$ dependency and we want to use the current center for the simple one-dimensional case on the X_1-axis of Fig. 1. The two equal currents $I/2$ at a distance d on the X_1-axis are replaced by a single one of double intensity (on the X_2-axis) at the current center, which is located at a distance r from the origin. The relative error for this particular case can then be shown to be equal to

$$\left|\frac{E_o - E_e}{E_o}\right| = \frac{d^2}{4r^2 - d^2}. \tag{3}$$

In which E_o is the field at the origin caused by the original distribution and E_e is the field caused by the equivalent, placed at the current center. Equation (3) shows that the approximation will improve when the distance/size ratio goes to infinity. As the component size gets larger compared to the distance between the components, the approximation becomes worse.

Another factor that will influence the accuracy of the dipole model is the size of the component relative to the wavelength. If the excitation frequency increases, then the current distribution on the component will become more complex, needing more dipoles to be modeled accurately.

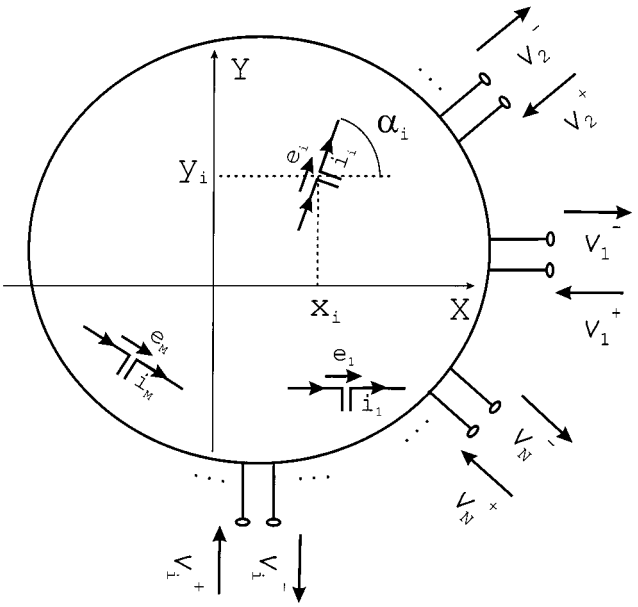

Fig. 2. General N-port using M elementary dipoles to model radiation behavior.

III. Extension of the S-Parameter Model

In this section, we will explain how, for a general discontinuity (with an arbitrary number of ports and an arbitrary number of dipoles), the S-parameter model for the discontinuity can be extended to include the effects of mutual coupling in the circuit calculations.

In general, an incident waves on a port of a discontinuity will cause outgoing waves on the ports and current distributions, differing for each port of incidence, within the volume of the discontinuity. The current distribution within the component will generate incident fields on the other discontinuities of the circuit, which will cause outgoing waves on the ports of these other discontinuities. Fig. 2 shows a general N-port, which uses M dipoles to model the radiation behavior that is caused by the current distributions.

The dependence of the outgoing port waves (v_i^-) on the incident port waves (v_i^+) within one discontinuity is described by the S-parameter description of the discontinuity. This dependence is shown for a general N port in the following:

$$\begin{bmatrix} v_1^- \\ v_2^- \\ \vdots \\ v_N^- \end{bmatrix} = \begin{bmatrix} s_{11} & s_{12} & \cdots & s_{1N} \\ s_{21} & s_{22} & \cdots & s_{2N} \\ \vdots & \vdots & & \vdots \\ s_{N1} & s_{N2} & \cdots & s_{NN} \end{bmatrix} \begin{bmatrix} v_1^+ \\ v_2^+ \\ \vdots \\ v_N^+ \end{bmatrix} \tag{4}$$

where s_{ii} is the reflection coefficient at port i and s_{ij} is the transmission coefficient from port j to port i.

The description only takes the fundamental transmission-line mode into account. This implies that, at the reference plane of the S-parameter port, the higher order modes must have died out. If needed, a piece of transmission line of sufficient length must be added to the component to satisfy this condition.

The dependence of the outgoing port waves of one discontinuity on the incident port waves of another one is calculated by extending the S-parameter description as described below.

First, data is added that links the incident port waves (v_i^+) to the currents of the dipole model (v_i) through the T matrix in the following:

$$\begin{bmatrix} i_1 \\ \vdots \\ i_M \end{bmatrix} = \begin{bmatrix} t_{11} & \dots & t_{1N} \\ \vdots & \ddots & \vdots \\ t_{M1} & \dots & t_{MN} \end{bmatrix} \begin{bmatrix} v_1^+ \\ \vdots \\ v_N^+ \end{bmatrix} \tag{5}$$

where t_{mn} is the current on dipole m, caused by a 1-V incident wave at port n. The relation between the longitudinal component of the incident fields on the dipoles (e_i) and the outgoing waves (v_i^-) at the ports is then described through the R matrix as follows:

$$\begin{bmatrix} v_1^- \\ \vdots \\ v_N^- \end{bmatrix} = \begin{bmatrix} r_{11} & \dots & r_{1M} \\ \vdots & \ddots & \vdots \\ r_{N1} & \dots & r_{NM} \end{bmatrix} \begin{bmatrix} e_1 \\ \vdots \\ e_M \end{bmatrix} \tag{6}$$

where r_{nm} is the amplitude of the outgoing wave at port n for a 1-V/m incident field at dipole m. The full new extended description for the discontinuity then becomes

$$\begin{bmatrix} V^- \\ I \end{bmatrix} = \begin{bmatrix} S & R \\ T & X \end{bmatrix} \begin{bmatrix} V^+ \\ E \end{bmatrix}. \tag{7}$$

In which S is the S-parameter matrix, and R and T are the matrices defined in (6) and (5). The X submatrix describes the reflections of incident fields at the dipole model's dipoles. Due to these reflections, indirect paths can be formed between two discontinuities through other discontinuities. The additional fields that are caused by these indirect paths are assumed to be small compared to the field caused by the direct path. Therefore, the influence on the S-parameters of the global circuit of these reflections at discontinuities is negligible and the elements of the X submatrix can be set to zero. The results in the numerical result section prove the validity of this assumption.

The relation between the currents on one discontinuity's dipoles and the incident fields on another's discontinuity's dipoles is given by the appropriate Green's functions. The field distribution for a dipole, positioned at the origin, is derived from the current and charge Green's function using the mixed-potential expression that is described in [1]. In [1], it is shown that the field, caused by a current distribution $\vec{K}^e$, can be written as

$$\vec{E}(x,y) = \int_{x'}\int_{y'} g_j(r)\cdot\vec{K}^e(x',y')dx'dy' + \vec{\nabla}\int_{x'}\int_{y'} g_q(r)\left(\vec{\nabla}'_t\cdot\vec{K}^e(x',y')\right)dx'\,dy' \tag{8}$$

in which (x,y) is the observation location, (x',y') are the source coordinates, r is the distance between source and observation, g_j is the Green's function for current sources, and g_q is the Green's function for charge sources. If the X-dipole is modeled as two charges at an infinitesimally small distance dx, with a current I with unit amplitude flowing between them, then the x-dipole's x- and y-field distributions can be derived from (8)

$$\begin{aligned} G_x(x,y) &= g_j(r) + \frac{g_q''(r)x^2}{r^2} + \frac{g_q'(r)y^2}{r^3} \\ G_y(x,y) &= \frac{g_q''(r)xy}{r^2} - \frac{g_q'(r)xy}{r^3}. \end{aligned} \tag{9}$$

The relations between the current on one dipole and the field it causes on another one can be written as a matrix equation for each combination of two discontinuities

$$E_i = G_{i,j}I_j. \tag{10}$$

In which E_i is the vector containing the incident fields on the dipoles of the ith discontinuity and I_j is the vector containing the currents on the dipoles of the jth discontinuity.

By using the additional dipole data in (5), (6), and (10), and the S-parameter description of (4), we are now able to describe the circuits discontinuities including their interaction by mutual coupling as one big S-matrix. This is shown in (11), at the bottom of this page, for a circuit containing D discontinuities. All the elements are (sub)matrices themselves. They describe the direct paths between the discontinuities.The new matrix will be named S_d. Its number of ports is equal to the total number of ports, summed over all the circuit's discontinuities. Equation (11) is only valid when the X submatrix in (7) is set to zero. If this is not the case, then the submatrices will become infinite sums over the direct path and all the indirect paths. The circuit would then have to be solved by a full matrix inversion, keeping the dipole currents and fields as unknowns. This would slow the method down considerably.

The S_d matrix describes all the discontinuities and their mutual interaction through radiation as a single big S-port network. All the ports of the discontinuities in the circuit (except the externally fed ones) are connected through transmission lines. The S-parameter description (normalized to the characteristic impedance of the line) for a transmission-line connection is

$$\begin{bmatrix} v_1^- \\ v_2^- \end{bmatrix} = \begin{bmatrix} 0 & e^{-j\gamma l} \\ e^{-j\gamma l} & 0 \end{bmatrix} \begin{bmatrix} v_1^+ \\ v_2^+ \end{bmatrix}. \tag{12}$$

Where γ is the propagation constant of the line and l is its length. By renormalizing the port impedances of the transmission lines

$$\begin{bmatrix} V_1^- \\ \vdots \\ \\ \\ \vdots \\ V_D^- \end{bmatrix} = \begin{bmatrix} S_1 & R_1G_{1,2}T_2 & R_1G_{1,3}T_3 & \dots & R_1G_{1,D}T_D \\ R_2G_{2,1}T_1 & S_2 & R_2G_{2,3}T_3 & \dots & R_2G_{2,D}T_D \\ \vdots & & \ddots & & \\ R_DG_{D,1}T_1 & \dots & R_DG_{D,D-1}T_{D-1} & & S_D \end{bmatrix} \begin{bmatrix} V_1^+ \\ \vdots \\ \\ \\ \vdots \\ V_D^+ \end{bmatrix} \tag{11}$$

to the corresponding port impedance of the connected discontinuity port and inserting the transmission line (12) into (11), we can eliminate all the unknown waves at the ports that are connected through transmission lines. What remains is an S-parameter description for the entire circuit between its externally excited ports. This description includes the mutual coupling between the discontinuities, but not between discontinuities and transmission lines and between transmission lines. These couplings are calculated using another procedure, which is implemented within separate modules. These procedures are not the topic of this paper, but are described in [7] and [8].

IV. Determination of Optimal Dipole Positions and T and R Matrices for Dipole Model

In this section, two procedures will be described to calculate the T and R matrices of the above-described S-parameter extension and the optimal positions for the dipoles that model the radiation behavior. We assume that the optimal dipole positions do not change much as a function of frequency so that they can be calculated at a fixed frequency.

Both methods use the field that the discontinuity generates to calculate the optimal dipole positions. The advantage of starting from the field is that this field can either be calculated (using a MoM if the current distribution is known) or be measured in a test setup such as the one described in [9] (if the current distribution is not known). Measurements can be used for packaged components with unknown internal geometry. Calculations are possible if the component's internal structure is entirely known (e.g., monolithic-microwave integrated-circuit (MMIC) components).

As was mentioned in Section II, the Green's functions for a multilayer substrate can be quite complex. Therefore, it is not easy to use an analytical method to calculate the ideal dipole positions from the current distribution and the Green's function.

A first method uses the correlation function of the field generated by a dipole and the field generated by the current distribution in the substrate. This correlation function is shown in the following:

$$C(x',y',z',\alpha') = \int_x\int_y\int_z \vec{E}_{\text{disc}}(x,y,z) \times \vec{E}_{\text{dip}}(x-x',y-y',z-z',\alpha')dxdydz. \tag{13}$$

$\vec{E}_{\text{disc}}$ and $\vec{E}_{\text{dip}}$ are the fields generated by the discontinuity and the dipole when they are placed at the origin. α' is the angle at which the dipole is positioned. The maximum of this correlation function yields the position (x',y',z') and orientation (α') at which the dipoles field will exhibit most similarity to the field generated by the current distribution. By subtracting the field of the dipole at this position from $\vec{E}_{\text{disc}}$ and using (13) again on the remaining field, other dipoles can be extracted, improving the similarity between the fields produced by the model and by the original current distribution.

The second method uses an optimization procedure to position and excite N_d X-, Y-, or Z-oriented dipoles in such a way that their combined field resembles the field produced by the current distribution as closely as possible in N_t test points that are positioned in a circle with radius R_t around the current distribution. To do this, the optimization procedure will need to adjust $5\times N_d$ input parameters (x, y, and z positions and complex excitation for the dipoles) to optimize $6\times N_t$ output parameters (complex X, Y, and Z components of the fields in each test point). The relation between the N_d dipole excitations i_n and the fields in the N_t test points $E_{\text{dip}}(m)$ (for given dipole positions) is given by the following linear set of equations:

$$\begin{aligned} &Z_{1,1}i_1 + Z_{1,2}i_2 + \cdots + Z_{1,N_d}i_{N_d} = E_{\text{dip}}(1)\\ &Z_{2,1}i_1 + Z_{2,2}i_2 + \cdots + Z_{2,N_d}i_{N_d} = E_{\text{dip}}(2)\\ &\vdots\\ &Z_{N_t,1}i_1 + Z_{N_t,2}i_2 + \cdots + Z_{N_t,N_d}i_{N_d} = E_{\text{dip}}(N_t) \end{aligned} \tag{14}$$

in which Z is a matrix that describes the relation between a current on a dipole and the field it causes in a test point. This means that, for given dipole positions (and, thus, certain values of Z), the optimal excitations can be calculated using a least square method in terms of the dipole positions. This leaves only the dipole positions $(3\times N_d)$ as input parameters. The output parameters (the fields in the test points: E_{dip}) are used to calculate a scalar cost function using (15). This cost function is the sum of the squared differences between the current dipole models fields (E_{dip}) and the original discontinuity's fields (E_{disc})

$$Cst\left(x'_1,y'_1,z'_1,\ldots,x'_{N_d},y'_{N_d},z'_{N_d}\right) = \sum_{n=1}^{N_t}\left(E_{\text{disc}}(n) - \sum_{m=1}^{N_d} Z_{n,m}i_m\right)^2 \tag{15}$$

in which (x'_m,y'_m,z'_m) is the position of the mth dipole and i_m is the current on the mth dipole that was calculated using the least square method. The current distribution on the discontinuity will be different for each port of the discontinuity that is excited. The total cost is the sum of the costs for each distribution (port). This means that the dipole positions that are optimal, in a mean sense, for all the distributions at the same time are searched for.

The starting positions of the dipoles for the optimization are calculated using the current center and the spreading of the current distributions. If one dipole is used it is placed at the center, two dipoles are placed at the center $\pm$ the spreading and three dipoles are placed at the center $\pm$ the spreading and one at the center. This is done for the x- and y-oriented dipoles separately. For the x dipoles, the x-oriented current distribution is used and vice versa. If more than three dipoles (per current component) are used, than the starting positions can be chosen manually or the points where the current distribution derivative changes sign (maxima) can be used. Other methods ([10] and [11]) can be used to find good starting points starting from the current distribution.

The number of dipoles that are needed to model the discontinuity with enough accuracy increases if: 1) the discontinuity's complexity increases; 2) the discontinuity becomes bigger relative to the wavelength; and 3) the discontinuity becomes bigger relative to its distance to the other components. The examples

in the numerical section give a general idea about the number of dipoles that have to be used. A very coarse rule could be one dipole for every 18 basis functions of the MoM. The quality of the model can be checked immediately after the optimization procedure from the correlation and error graphs shown in Section V. If the distance between the discontinuities becomes very small and the coupling between the discontinuities becomes high, then the shape of the current on the discontinuities starts to change. At this point, adding more dipoles will not improve the results any more because a fundamental assumption of the dipole model (that the second-order coupling can be neglected) is not valid any more. The maximum allowable coupling levels at which second-order coupling can still be neglected are described in [7] and [8].

The optimization itself is an iterative process involving the following two steps.

Step 1) Calculate the gradient of the cost function (a function of the dipole positions) at the starting point.

Step 2) Perform a one-dimensional optimization to find the optimal point along a line that goes through the starting point and has a direction given by the gradient.

After step 2, step 1 is repeated with the new optimal positions as starting positions. These steps are repeated until the cost becomes stable.

The T matrix (the dipole excitations for each port) is recalculated for each frequency in the frequency list of the model. This is done using the least square method while keeping the dipoles fixed at their earlier (at the midband frequency) optimized positions. Changing the frequency will result in changing the Z coupling coefficients in (14).

It can be proven that the R matrix can easily be deduced from the T matrix through reciprocity. Since the shape of the pattern should be the same for transmission and receiving, we can say that the elements of the R and T matrix must be the same, except for a constant factor that we will call the receiving constant $R_{\rm cte}$

$$[R] = R_{\rm cte} \cdot [T]. \tag{16}$$

We can now write the coupling between two random different dipole models (discontinuities) the first dipole model has I dipoles and the second one has J dipoles. For S_{12}, we get

$$S_{12} = R_{\rm cte1} \sum_{i=1}^{I} T_1(i) \left(\sum_{j=1}^{J} G(i,j) T_2(j) \right). \tag{17}$$

S_{21} is equal to

$$S_{21} = R_{\rm cte2} \sum_{j=1}^{J} T_2(j) \left(\sum_{i=1}^{I} G(j,i) T_1(i) \right). \tag{18}$$

Due to reciprocity, S_{12} is equal to S_{21}^T and $G(i,j)$ is equal to $G(j,i)$. The double summation in (18) can be rearranged so that it is equal to the double summation of (17). Therefore, $R_{\rm cte1}$ must be equal to $R_{\rm cte2}$. Since we used two arbitrary dipole models, $R_{\rm cte}$ must be a universal constant, which has the same value for every possible dipole model. To calculate the value of this constant, we can now choose the easiest possible case.

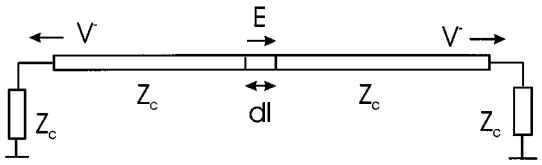

Fig. 3. Equivalent circuit for the calculation of $R_{\rm cte}$.

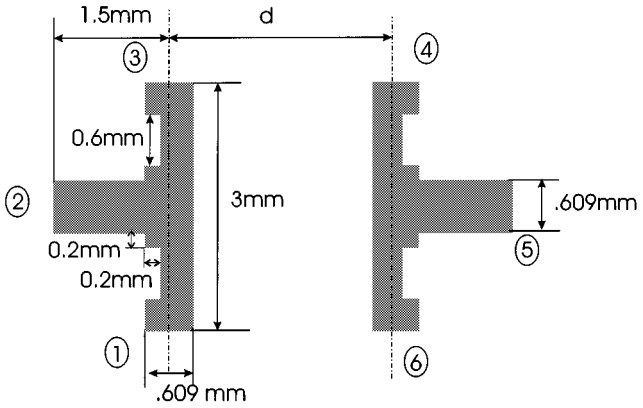

Fig. 4. Two T-junctions used to check the method.

This case is shown in Fig. 3. The "discontinuity" that we are going to model is just a piece of transmission line with infinitesimally small length dl, which is fed at both ends by two equally wide transmission lines with a characteristic impedance of Z_c. We choose Z_c equal to 1 Ω. The outgoing waves (V^-) for a certain incident field (E) will then be equal to

$$V^- = \frac{dl\, E}{2}. \tag{19}$$

If we would model this piece of transmission line by a horizontal dipole, then its excitation coefficient (t_{11}) would be equal to dl. Therefore, we can conclude that $R_{\rm cte}$ is equal to 1/2.

V. Numerical Results

The method described above is tested for the simple case of two shaped T-junctions. This structure is shown Fig. 4. A three- and a six-dipole model are calculated for this discontinuity and the fields generated by the models are compared to those of the component as a function of frequency and distance. The calculated model is then used to calculate the S-parameters for the two coupled T-junctions.

The T-junctions are placed on a substrate with $\varepsilon_r = 9.9$ and a thickness of 0.631 mm. For this substrate, the lines have a characteristic impedance of 50 Ω. The results of the new method will be compared to those of the normal MoM. Both T-junctions are then segmented using a square mesh of 0.2 $\times$ 0.2 mm segments (3 mm/15), which will generate 88 unknowns (rooftop basis functions).

Using the optimization technique described in Section IV, a dipole model is calculated for this T-junction in a frequency band of 1–30 GHz. In all the following figures, the T-junction or its model is placed as shown in Fig. 5. The continuous line in the figures refers to the x-oriented fields and the dashed line refers to the y-oriented fields.

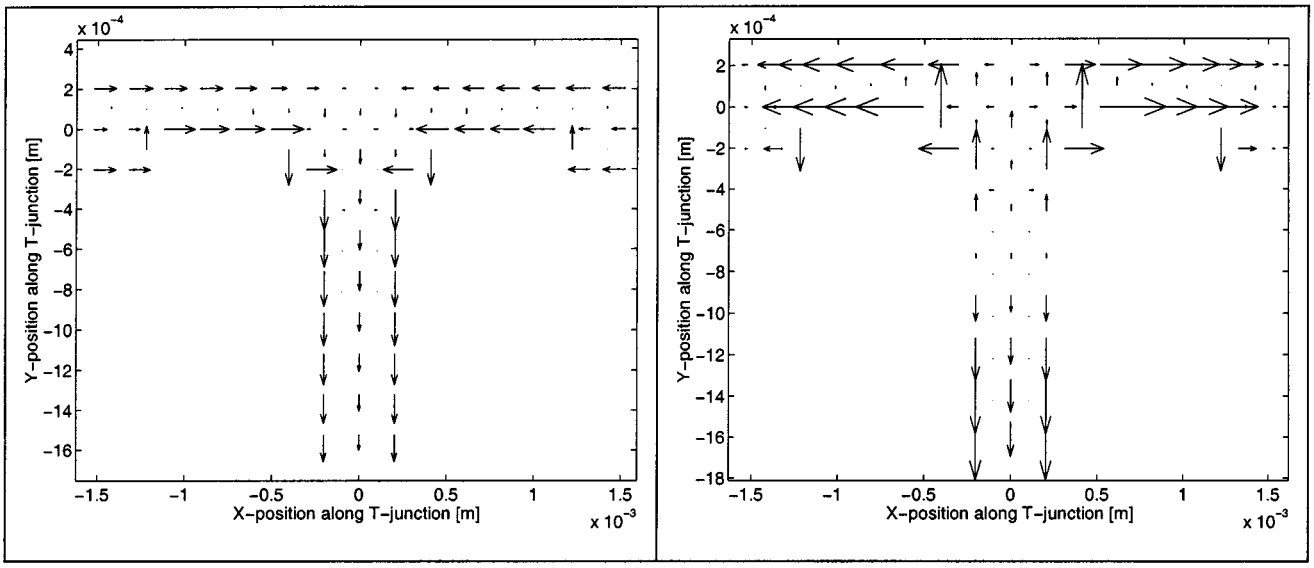

Fig. 5. Current distribution (rooftops) for T-junction excited at middle port at 5 GHz (left-hand side) and 30 GHz (right-hand side).

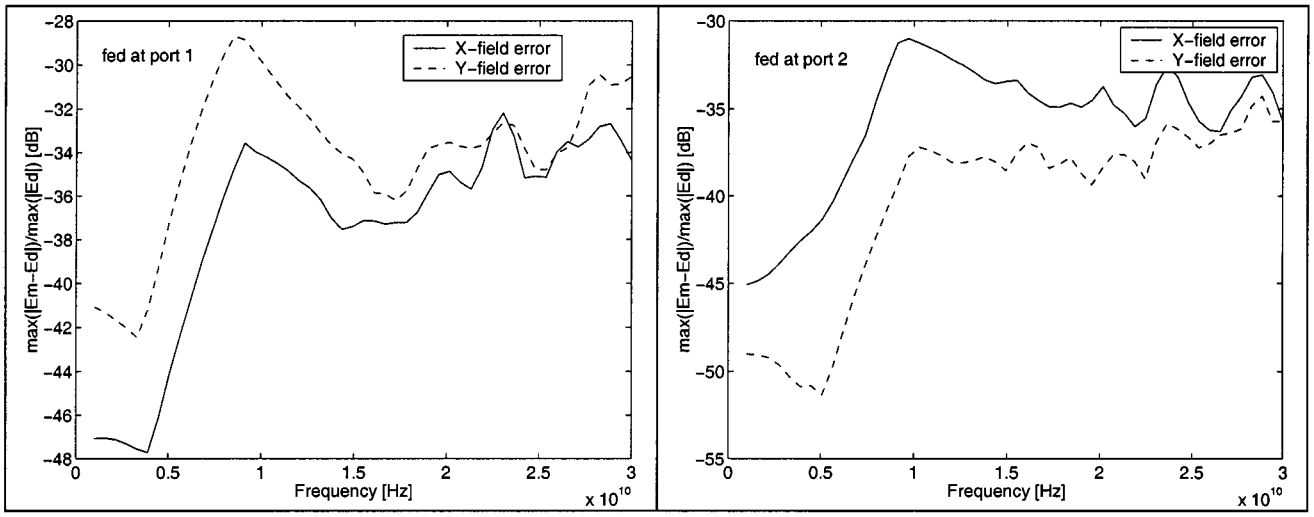

Fig. 6. Ratio of maximum error to maximum field value for excitation at ports 1 (left-hand side) and 2 (right-hand side). Six-dipole model. Frequency scan at 4 mm.

At the start of the optimization procedure, with the six dipoles, initial position set by the current center and the current spread as was described in Section IV, the cost, given by (15), is equal to 177. The optimization of the dipole positions reduces this to 32. The current distributions on the T-junction when excited at port 2 at 5 and 30 GHz are shown in Fig. 5. Each arrow represents a basis function. At 30 GHz, the wavelength is about equal to the component's size (3 mm) and the current is varying because of the phase differences across the length. This implies that we will need more dipoles to model the component at this frequency. The first model uses six dipoles. It is verified by comparing the field it generates at the test points to the original field distribution. This is shown as a function of frequency in Fig. 6. The 100 test points are placed in a circle of 4 mm around the center of the model. The graphs show the ratio of the maximum error (over all the test points) to the maximum field strength (over all the test points). The frequency at which the dipole positions are optimized is 5.5 GHz, which is (logarithmically) at the middle of the frequency band. The same can now be done for a fixed frequency as a function of the observation distance. This is shown in Fig. 7 for the lowest frequency (1 GHz). As can be expected, the correlation is worst at close range and is maximum when the distance is equal to the radius of the test-point circle because the model was optimized for this distance. At larger distances, the ratio of maximum error to maximum field strength goes to a steady value of -30 dB. The fluctuations in the curve at greater distances are due to numerical problems with the Green's function. At greater distances, the derivatives of the Green's function, needed in (9), become very small. Therefore, they become dominated by numerical noise. The solution for this is to use more points for the interpolation of the Green's function, but this increases the computation time. The worst result is obtained when the frequency and distance are the lowest. Fig. 8 shows a polar plot at 2 mm and 1 GHz to illustrate this. The continuous line represents the original field and the "+" line represents the

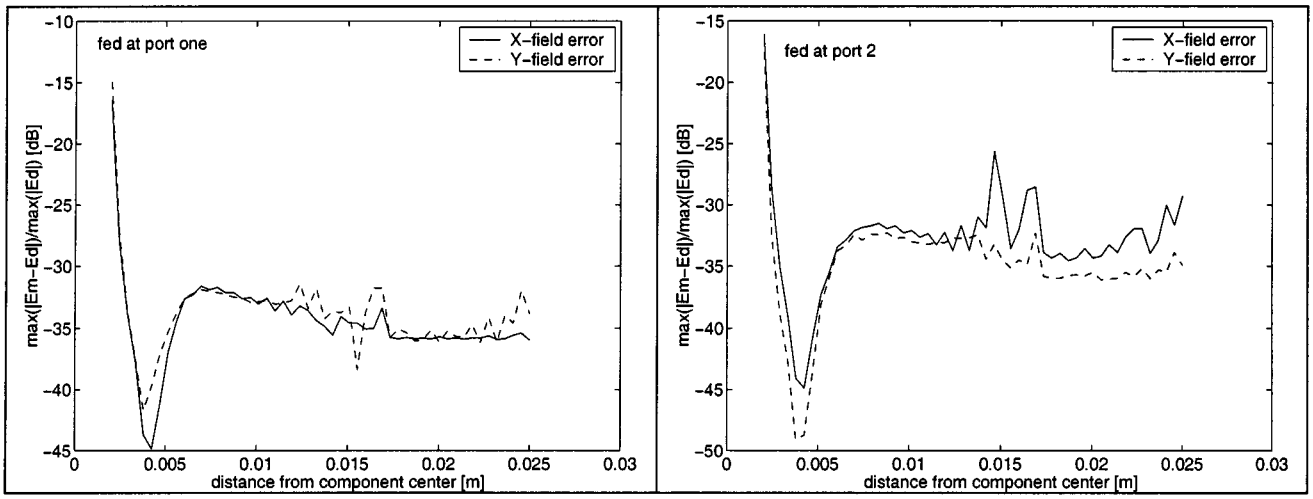

Fig. 7. Ratio of maximum error to maximum field value for excitation at ports 1 (left-hand side) and 2 (right-hand side). Six-dipole model. Distance scan at 1 GHz.

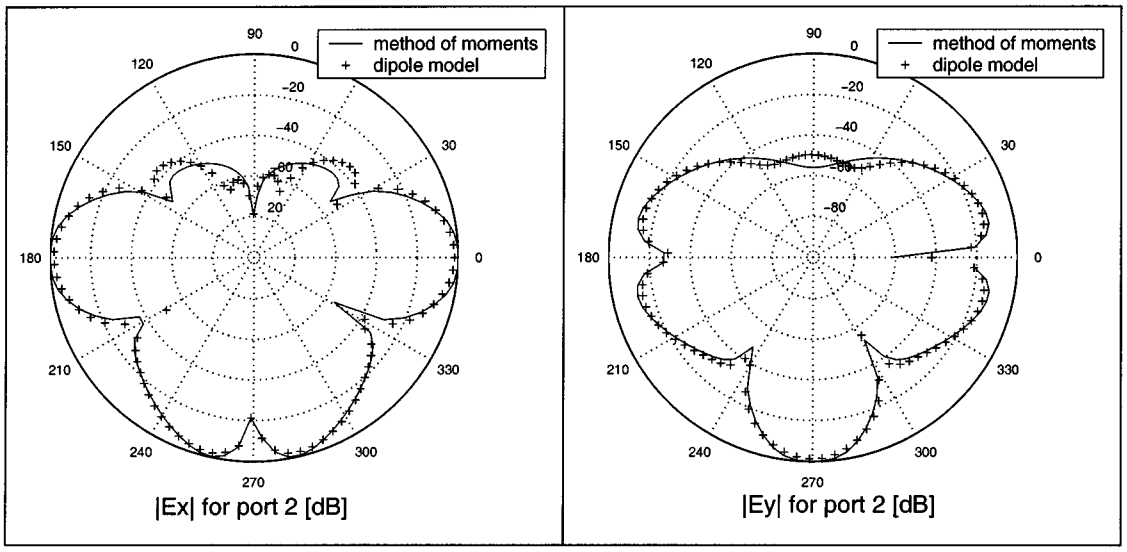

Fig. 8. Polar scan of six-dipole T-junction model, compared to original field, at 2 mm and 1 GHz.

model's field. The left-hand side of the figure is the X-oriented field and the right-hand side shows the Y-oriented field.

For higher frequencies, the results become better: the error ratio is below -35 dB for each port above 4 mm at 30 GHz. The reason for this is that the feeding charges that appear at the ports of the T-junction become smaller as the frequency increases. The current at a port is equal to the time derivative of the feeding charge. Therefore, the needed feeding charge becomes smaller for increasing frequency and constant current amplitude. The feeding charges make it harder to model the component's radiation pattern; hence, the decreasing model quality at lower frequencies. At even higher frequencies, the model will fail because the phase variation across the discontinuity cannot be modeled accurately enough with the six dipoles, the answer to this problem is to increase the number of dipoles. This problem is illustrated in Fig. 9 by using a three-dipole model (one dipole for each leg of the T-junction) for the T-junction. The test points for the optimization of the three-dipole model are placed at a

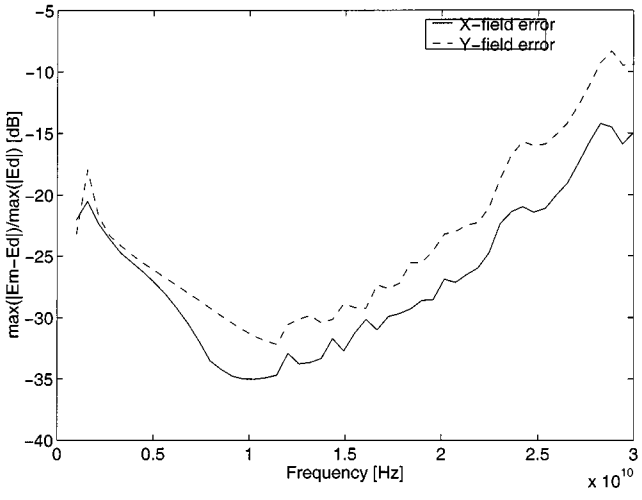

Fig. 9. Frequency dependency of the error ratio for the middle line for a three-dipole model with test points at 9-mm distance.

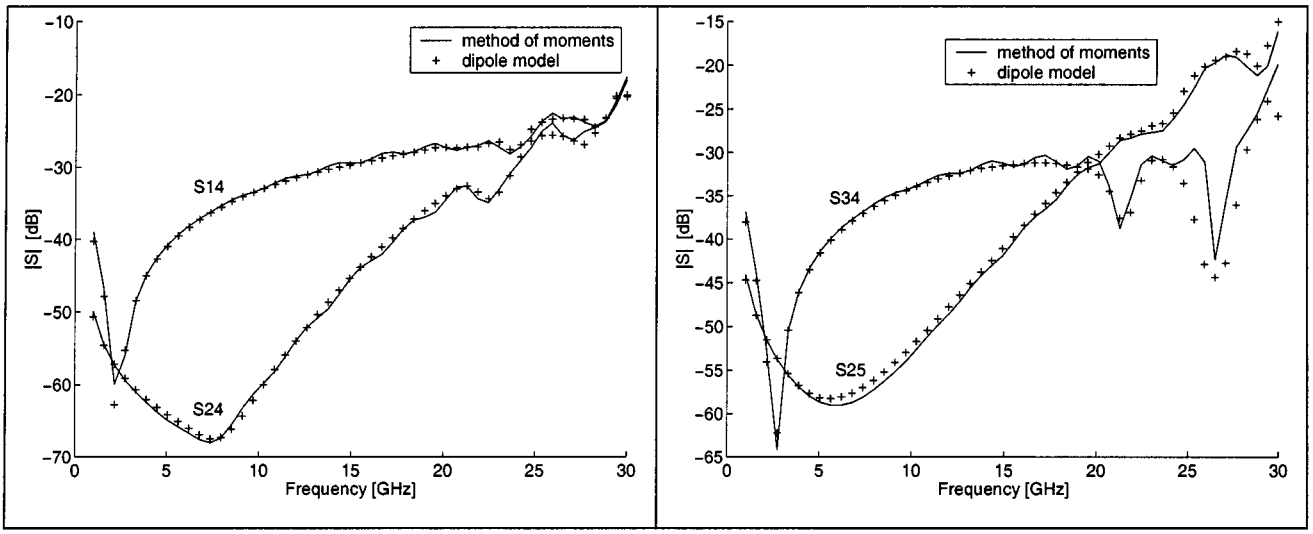

Fig. 10. S-parameters for the structure shown in Fig. 4. The continuous line was calculated using the MoM. The "+" line is calculated using the six-dipole model.

larger distance (9 mm) because, at 4 mm, no good result can be obtained using only three dipoles. As the frequency increases, the results clearly deteriorate.

The model shown in Figs. 6–8 will now be used to calculate the mutual coupling between the two T-junctions, as depicted in Fig. 3. The ports are numbered as indicated on this figure. The calculation is for a distance $d = 3$mm. Fig. 10 shows the S-parameters for this case, obtained with the dipole model ("+" line), compared to the solution with the moment method (continuous line).

The sharp increase in the coupling levels at the lowest frequencies is caused by the earlier mentioned feeding charges that feed the current at the positions of the ports. As explained before, these charges will become bigger as the frequency decreases and raise the coupling levels. If the component is fed by lines (these were not taken into account here), then the feeding charges of the component and the feeding charges of the lines that are feeding it will cancel out.

The last example handles a more complex structure. The structure is a shunt series resonator, placed on a substrate with a thickness of 1.2 mm and a relative permittivity of 2.2. The first (wanted) resonance is at 4.2 GHz and results in a dip of -25 dB in S_{12} . A second (parasitic) resonance occurs at 7.5 GHz. Two of these resonators are positioned as shown in Fig. 11 (the resonator on the right has been rotated 180°). The port numbering of this four-port is shown in this figure. The structure is about 10 × 10 mm (about one-quarter of a wavelength at 8 GHz). The distance between the outer edges of the two resonators is 5 mm. The coupling between the two shunt resonators is calculated using 17 dipoles per resonator for the dipole model and using 340 (rooftop) basis functions per resonator for the MoM. The model is first tested separately, again by plotting the maximum error to maximum field ratio. The graphs on the right-hand side of Fig. 12 show the ratio at 4.2 GHz, fed at ports 1 and 2, as a function of the distance from the center of the model. The graphs on the left-hand side show the ratio as a function of frequency at 12 mm from the center of the model. Fig. 13 shows the coupling from ports 3 to 1 and

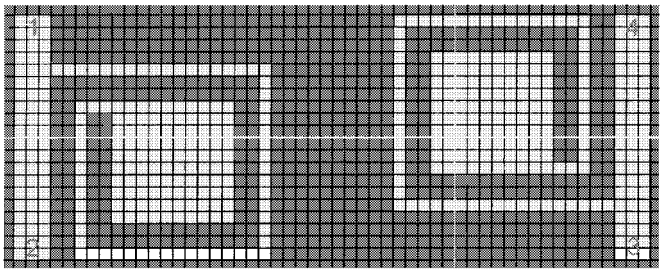

Fig. 11. Two shunt series resonators composing a four-port. Each segment is 0.5 × 0.5 mm.

from ports 4 to 1, calculated with the dipole model and using the MoM. The maximum error is about 1.5 dB and 7°. This is still a good result because this is a very difficult situation due to the following.

1) The component is large compared to the wavelength and compared to the distance between the components.
2) The component is actually a circuit in itself, which contains about seven discontinuities.
3) The component is very frequency selective and the optimal dipole positions are only calculated for one frequency (in this case, 4.2 GHz). The optimal dipole excitations are recalculated for each frequency though.

To illustrate the speed difference between the regular MoM and the dipole model calculations, we will now try to estimate the number of floating point operations (flops) as a function of the number of components in the circuit for both methods. To do this, we must first assume a few "typical" values for a component. N_{upc}, the typical number of basis functions per component, is set to 50. N_d, the typical number of dipoles per component is set to six. N_p, the typical number of ports per component, is set to two. The number of flops needed to couple N_c components using the dipole model is then given by

$$\text{flops} = \frac{N_c(N_c-1)}{2}\left(N_d^2 + 2N_dN_p\right). \tag{20}$$

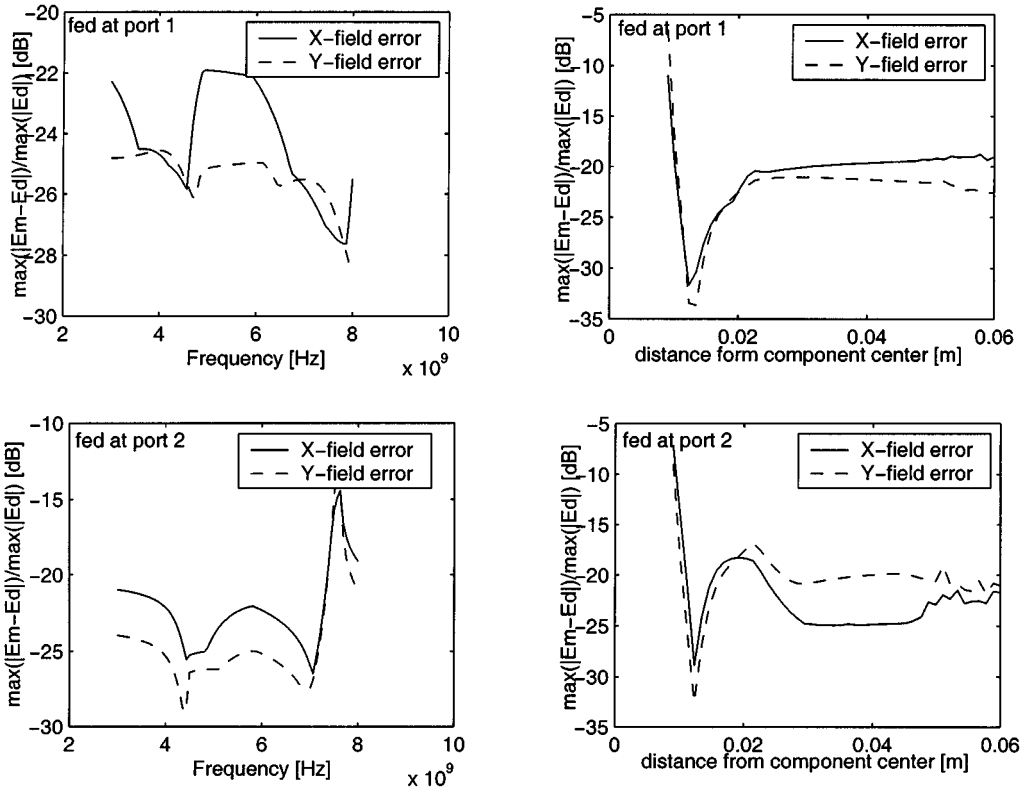

Fig. 12. Maximum error to maximum field ratio for a series resonator of Fig. 11. Left-hand-side graphs: ratio as a function of frequency at 12 mm from the center of the model, right-hand-side graphs: ratio as a function of distance at 4.2 GHz. Upper graphs: port 1 fed, lower graphs: port 2 fed.

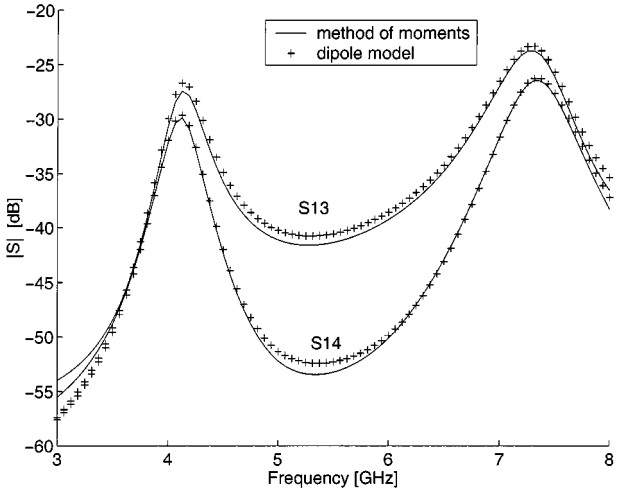

Fig. 13. Comparison of S_{13} and S_{14} for the two resonators calculated using the dipole model $(+)$ and using MoM (continuous line).

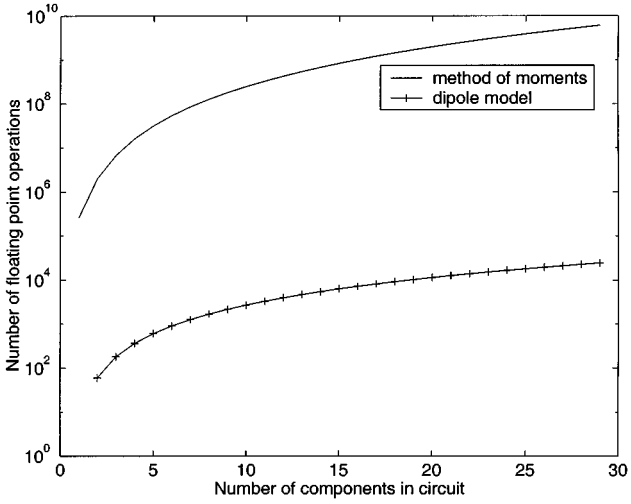

Fig. 14. Comparison of the needed number of floating point operations for MoM $(+\mathrm{line})$ and for the dipole model (continuous line) as a function of the number of components in the circuit.

The number of flops needed to solve the integral equations is more or less proportional to N_{tu}^3, where N_{tu} is the total number of unknowns $(N_{\mathrm{tu}} = N_c N_{\mathrm{upc}})$. To get a more accurate estimate, we used the flops command in Matlab to get the exact number of flops needed to solve the matrix. The number of flops needed for both methods is compared in Fig. 14. It is clear that the method proposed in this paper needs significantly less flops than the MoM, especially for larger circuits. From (20), we can also conclude that the calculation time increases proportional to the square of the mean number of dipoles that is used in the components, whereas in the MoM, it increases proportional to the third power of the number of basis functions that is used. It must also be noted that a separate "dipole Green's function" can be used that contains the coupling between dipoles as a function of distance, whereas the coupling between basis functions always involves integrating the Green's function over the source and observation basis functions. This results in a further speed up of the described method over the MoM.

VI. Conclusions

The main advantage of this method is the speed up: for the first example, the MoM uses 2.142 s to set up its matrix, 0.345 s to solve it, and 3.427 s to deembed the six ports. The same machine (HP C-160 160-MHz risc processor) needs only 0.152 to calculate the dipole couplings and the corresponding S-parameters. For large circuits, the speed up will become much bigger because the inversion time will rise proportional to the third power of the number of unknowns. The dipole model needs no matrix inversion and will work much faster for large circuits.

Another advantage is that the dipole model needs much less memory than the moment method because only the couplings between the dipoles of two discontinuities need to be kept in memory. It has been demonstrated in this paper that, for the coupling situations that arise between components in a regular circuit, the new method is accurate enough (max. 1.5-dB deviations) to be used for the design of circuits.

References

[1] G. A. E. Vandenbosch and A. R. Van de Capelle, "Mixed-potential integral expression formulation of the electric field in a stratified dielectric medium—Application to the case of a probe current source," *IEEE Trans. Antennas Propagat.*, vol. AP-40, pp. 806–817, July 1992.

[2] ——, "Accurate modeling tool for coaxially fed microstrip patch configurations in stratified dielectric media," *Arch. Elektron. Ubertrag.*, vol. 49, no. 3, pp. 151–159, Mar. 1995.

[3] B. L. A. Van Thielen and G. A. E. Vandenbosch, "MAGMAS: Present status," in *Proc. COST 245 ESA Workshop Active Antennas*, Noordwijk, The Netherlands, June 1996, pp. 149–159.

[4] F. J. Demuynck, G. A. E. Vandenbosch, and A. R. B. Van de Capelle, "The expansion wave concept—Part I: Efficient calculation of spatial Green's functions in a stratified dielectric medium," *IEEE Trans. Antennas Propagat.*, vol. 46, pp. 397–406, Mar. 1998.

[5] ——, "The expansion wave concept—Part II: A new way to model mutual coupling in microstrip arrays," *IEEE Trans. Antennas Propagat.*, vol. 46, pp. 407–413, Mar. 1998.

[6] R. Coifman, V. Rokhlin, and S. Wandzura, "The fast multipole method for the wave equation: A pedestrian prescription," *IEEE Antennas Propagat. Mag.*, vol. 35, pp. 7–12, June 1993.

[7] B. Van Thielen and G. A. E. Vandenbosch, "Method for the acceleration of transmission-line coupling calculations," *IEEE Trans. Microwave Theory Tech.*, vol. 49, pp. 1531–1536, Sept. 2000.

[8] ——, "Fast transmission line coupling calculation using a convolution technique," *IEEE Trans. Electromagn. Compat.*, vol. 43, pp. 11–17, Feb. 2001.

[9] K. Yang, G. David, J.-G. Yook, I. Papapolymerou, L. P. B. Katehi, and J. F. Whitaker, "Electrooptic mapping and finite-element modeling of the near-field pattern of a microstrip patch antenna," *IEEE Trans. Microwave Theory Tech.*, vol. 48, pp. 288–295, Feb. 2000.

[10] B. Truyden and J. Cornelis, "Adiabatic layering: A new concept of hierarchical multi-scale optimization," *Neural Networks*, vol. 8, pp. 1373–1378, Aug. 1995.

[11] N. Dyn, D. Levin, and S. Rippa, "Numerical procedures for surface fitting of scattered data by radial functions," *SIAM J. Sci. Stat. Comput.*, vol. 7, pp. 639–659, June 1986.

Bart L. A. Van Thielen was born in Belgium, on May 8, 1970. He received the M.Sc. degree in electrical engineering from the Katholieke Universiteit Leuven, Leuven, Belgium, in 1996.

He is currently a Research and Teaching Assistant with the Telecommunications and Microwaves Section, Katholieke Universiteit Leuven. His research interests are mainly in the areas of electromagnetic theory, numerical methods, and electromagnetic compatibility.

Guy A. E. Vandenbosch (M'92) was born in Sint-Niklaas, Belgium, on May 4, 1962. He received the M.S. and Ph.D. degrees in electrical engineering from the Katholieke Universiteit Leuven, Leuven, Belgium, in 1985 and 1991, respectively.

From 1985 to 1991, he was a Research and Teaching Assistant with the Telecommunications and Microwaves Section, Katholieke Universiteit Leuven, where he was involved with the modeling of microstrip antennas with the integral equation technique. From 1991 to 1993, he held a post-doctoral research position at the Katholieke Universiteit Leuven. He is currently a Professor at the Katholieke Universiteit Leuven. His research interests are mainly in the area of electromagnetic theory, computational electromagnetics, planar and conformal antennas, and electromagnetic compatibility. He has authored or co-authored papers in international journals and has been presented at international conferences.

Prof. Vandenbosch is a member of the COST 260 Project, which is a European project on "smart antenna computer design and technology."